

Kernel-learning parameter prediction and evaluation in algebraic multigrid method for several PDEs

Junyue Luo, Xiaoqiang Yue, Fangfang Zhang, and Juan Zhang^{*}

Hunan Key Laboratory for Computation and Simulation in Science and Engineering, Key Laboratory of Intelligent Computing and Information Processing of Ministry of Education, School of Mathematics and Computational Science, Xiangtan University, Xiangtan, Hunan, China, 411105.

Abstract. This paper explores the application of kernel learning methods for parameter prediction and evaluation in the Algebraic Multigrid Method (AMG), focusing on several Partial Differential Equation (PDE) problems. AMG is an efficient iterative solver for large-scale sparse linear systems, particularly those derived from elliptic and parabolic PDE discretizations. However, its performance heavily relies on numerous parameters, which are often set empirically and are highly sensitive to AMG's effectiveness. Traditional parameter optimization methods are either computationally expensive or lack theoretical support. To address this, we propose a Gaussian Process Regression (GPR)-based strategy to optimize AMG parameters and introduce evaluation metrics to assess their effectiveness. Trained on small-scale datasets, GPR predicts nearly optimal parameters, bypassing the time-consuming parameter sweeping process. We also use kernel learning techniques to build a kernel function library and determine the optimal kernel function through linear combination, enhancing prediction accuracy. In numerical experiments, we tested typical PDEs such as the constant-coefficient Poisson equation, variable-coefficient Poisson equation, diffusion equation, and Helmholtz equation. Results show that GPR-predicted parameters match grid search results in iteration counts while significantly reducing computational time. A comprehensive analysis using metrics like mean squared error, prediction interval coverage, and Bayesian information criterion confirms GPR's efficiency and reliability. These findings validate GPR's effectiveness in AMG parameter optimization and provide theoretical support for AMG's practical application.

AMS subject classifications: 52B10, 65D18, 68U05, 68U07

Key words: Algebraic Multigrid method, Gaussian process regression.

^{*}Funding. The National Key R&D Program of China (2023YFB3001604).

^{*}Corresponding author. *Email addresses:* zhangjuan@xtu.edu.cn (Juan Zhang)

1 Introduction

We consider the sparse linear system defined by

$$Au = b, \tag{1.1}$$

where A is a non-singular matrix and b is a given vector. Solving this system is a cornerstone in scientific and engineering computing, particularly in the realm of elliptic partial differential equations (PDEs). These PDEs are notable for their ability to depict steady-state or equilibrium conditions. Notable instances include Laplace equation and Poisson equation, which are pivotal in modeling electric potential and gravitational fields, respectively. Numerically addressing such equations often leads to large-scale sparse linear systems, posing significant computational hurdles. Parabolic PDEs, which describe physical processes evolving over time, such as the heat conduction equation, also generate time-dependent linear systems. These systems necessitate the solution of sparse linear systems at each time step, similar to those arising in elliptic PDEs. The Helmholtz equation, a linear elliptic PDE with extensive applications in acoustics and electromagnetism, is particularly challenging due to its oscillatory solutions and the necessity for precise numerical handling of wave phenomena at each time step. In our numerical experiments, we concentrate on solving the following equations: the constant coefficient Poisson equation, the variable coefficient Poisson equation, the diffusion equation, and the Helmholtz equation. These equations encompass both temporal and spatial derivatives, resulting in a sequence of time-dependent linear systems. At each time step, a sparse linear system akin to that of an elliptic PDE must be tackled. Methods for solving such linear systems are broadly classified into direct and iterative approaches. Direct methods are favored for their high accuracy, stability, and predictability. However, their applicability is constrained when dealing with large-scale systems due to the prohibitive computational and storage requirements. Consequently, iterative methods have emerged as a vital tool for addressing large-scale sparse linear systems. Among these, the algebraic multigrid method (AMG) shines as an effective iterative technique for solving such systems.

In 1987, Ruge, J.W. and Stüben, K. [13] introduced the algebraic multigrid (AMG) method, an iterative algorithm tailored for efficiently solving linear algebraic equation systems. This method evolved from the theoretical foundations and principles of general multigrid methods. Unlike traditional methods, AMG does not require knowledge of the geometric and physical properties of the problem; it solely utilizes the information within the coefficient matrix of the linear system to construct a hierarchy of virtual grids. This capability allows multigrid techniques to be applied to a wide variety of problems, including those without a geometric context. The versatility and effectiveness of the AMG method have sparked extensive research interest, encompassing various aspects such as coarsening strategies, smoothers, and practical applications. The AMG parameters used in this paper will be explained in the section on numerical examples.

With the rise of machine learning, researchers have embarked on exploring the integration of AMG with machine learning techniques [26], or the utilization of machine learning to optimize the AMG method [1, 7, 15]. Our research extends this premise by striving to integrate machine learning methodologies with the AMG approach to augment its performance and applicability.

The effectiveness of the AMG method heavily relies on the selection of smoothing parameters. Traditionally, two main strategies have been employed to determine these parameters: systematic exploration of the parameter space through experimentation or empirical optimization, and theoretical estimation. While the first approach can yield highly accurate optimal parameters, it is time-consuming and often impractical in scientific computing due to the desire for a single, efficient computation. The second strategy, theoretical estimation, may provide a formula or algorithm for computing parameters, but it is problem-specific and any inaccuracies can significantly reduce algorithmic efficiency. Furthermore, as the size of the linear system increases, the applicability of theoretical methods may decrease, especially when it comes to selecting smoothing parameters. To address these challenges, we adopt the approach outlined in [10] and utilize Gaussian process regression (GPR) [24] to predict optimal parameters. We achieve this by training on a dataset derived from a smaller-scale system, which allows us to discern the mapping from the dimensions of the linear system to more optimal splitting parameters. This strategy avoids the costly parameter traversal and offers an efficient way to forecast relatively optimal parameters within practical computational settings. For the kernel function selection in the GPR method, we incorporate the kernel learning technique described in [4, 11]. This involves constructing a library of basic kernel functions and formulating the necessary kernel function as a linear combination of these components. The coefficients of this combination are determined through TDLS training. This approach not only simplifies the kernel function selection process but also enhances the accuracy of the predictive outcomes.

We have noticed some methods for evaluation metrics [6, 9, 17, 20, 27, 28], but they are merely based on one or a few evaluation indicators. Building upon this foundation, our research endeavors to address the limitations observed in prior studies regarding the evaluation of parameter prediction. We transcend the reliance on conventional metrics such as Mean Squared Error (MSE), Root Mean Squared Error (RMSE), and Mean Absolute Error (MAE) by introducing a suite of additional statistical measures. Specifically, we incorporate the R^2 score, also known as the coefficient of determination, which assesses the goodness of fit of our regression model and indicates the proportion of the dependent variable that is predictable from the independent variables. Furthermore, we utilize the correlation coefficient, a statistical measure that quantifies the strength and direction of the linear relationship between two variables. Additionally, we employ the Leave-One-Out cross-validation prediction error (LOO-SPE) to gauge the uncertainty associated with our model predictions. This method provides a robust assessment of model performance by evaluating predictions on each observation individually while using the remaining observations to train the model. Lastly, we incorporate the Bayesian Informa-

tion Criterion (BIC) value as a scoring criterion, which is useful for model selection by penalizing model complexity and preventing overfitting. By utilizing these comprehensive evaluation metrics, we are well-equipped to thoroughly assess the impact of parameter prediction across various combinations of kernel functions. This approach not only enhances the precision of our parameter predictions but also bolsters their reliability. Our research contributes to the field by providing a more nuanced understanding of parameter prediction in the context of AMG methods, ultimately paving the way for improved algorithmic performance and efficiency.

This paper proposes a Gaussian Process Regression (GPR)-based approach for predicting and optimizing parameters in Algebraic Multigrid (AMG) methods. The effectiveness of the proposed parameter selection strategy is demonstrated through numerical experiments on a series of partial differential equations (PDEs). The paper is structured as follows: Section 2 outlines the model and algebraic multigrid method, Section 3 details the GPR methodology for parameter prediction, Section 4 presents the results of numerical experiments on various PDEs, and Section 5 provides a comprehensive summary of our findings.

2 preliminary

The performance of the AMG method is closely related to the strong threshold parameter θ , which influences the final computational results and computational cost by determining the C/F splitting. Identifying appropriate parameters for this purpose poses a significant challenge. In this section, we first introduce the basic components of the AMG method, and then we present a novel approach to parameter selection using the GPR method. This method offers a data-driven alternative designed to reduce the computational overhead and enhance the reliability of parameter selection for the AMG method.

2.1 AMG algorithm

AMG methods are among the most efficient solvers for linear systems, whose core lies in alternately iterating between coarse and fine grids to handle different components of the error. Taking a two-level grid as an example: the process begins with performing a predefined number of pre-smoothing iterations on the fine grid to reduce high-frequency error components, followed by transferring the residual from the fine grid to the coarse grid via an interpolation operator for error correction, and finally prolongating the corrected residual back to the fine grid through a prolongation operator to update the iterative vector via post-smoothing, thereby achieving multi-level error reduction and accelerated convergence compared to single-grid methods.

The process can be divided into two stages: SETUP and SOLVE in AMG. In the SETUP phase, first input the strong threshold parameter θ , which is used to define the strong dependency set of variable i , as follows:

Definition 2.1. Given a strong threshold parameter $0 < \theta \leq 1$, the variable i strongly depends on the variable j if

$$|a_{ij}| \geq \theta \max_{k \neq i} |a_{ik}|.$$

Then we can define the strong dependency set S_i and strong influence set S_i^T of variable i ,

$$S_i = \{j \neq i : |a_{ij}| \geq \max_{k \neq i} |a_{ik}|, k = 1, 2, \dots, n.\},$$

$$S_i^T = \{j | i \in S_j\}.$$

Using criteria S_i and S_i^T and a specific coarsening strategy (such as the Ruge-Stüben algorithm), we partition the variables into a coarse set C and a fine set F . Detailed information can be found in [13]. Furthermore, we obtain the interpolation operator P and the lifting operator R , which will help us achieve the transfer of residuals between different grids.

During the SOLVE phase, we cycle between different grids using the components obtained from the SETUP phase. First, pre-smoothing is performed on the fine grid; subsequently, the obtained residuals are transferred to the coarse grid via the interpolation operator for exact solution; then, the corrected residuals are transferred back to the fine grid via the lifting operator for post-smoothing. We present the above two stages in the form of the following two algorithm tables.

Algorithm 1 SETUP phase

1. **Coarsening:** Construct the fine-level grid based on the matrix A and let Ω be the set containing all fine-level variables. Based on the input θ , partition set Ω into coarse grid variables C and fine variables F .
 2. **Computing A_c :** Based on the coarse variable set C , compute the interpolation operator P and lifting operator R . Then compute the coarse-level matrix A_c by $A_c = RAP$.
-

Algorithm 2 SOLVE phase

1. **Pre-smoothing:** smoothing k_1 iterations on $Ax = b$ get x^{k_1} .
 2. **Coarse-grid correction :**
 Restricting residuals into coarse grid : $b_c = R(b - Ax_k)$
 Obtain e^* by solving the coarse grid equation $A_c e = b_c$
 Interpolating and correcting: $x^{\text{new}} = x^{k_1} + P e^*$
 3. **Post-smoothing :** Perform k_2 iterations on the equation $Ax = b$ using x^{new} as the initial guess
-

2.2 Gaussian Process Regression

The training dataset is denoted as $D = \{(n_i, \theta_i) \mid i = 1, 2, \dots, d\} := \{\mathbf{n}, \theta\}$, where each pair (n_i, θ_i) is an input-output correspondence. In this context, n_i denotes the number of partitions, and θ_i signifies the connectivity parameters. Under the assumption that θ_i follows a Gaussian Process (GP) relative to n_i , the function evaluations $f(\mathbf{n}) = [f(n_1), f(n_2), \dots, f(n_d)]$ are collectively distributed as a d -dimensional joint Gaussian distribution (GD).

$$\begin{bmatrix} f(n_1) \\ \vdots \\ f(n_d) \end{bmatrix} \sim N \left(\begin{bmatrix} \mu(n_1) \\ \vdots \\ \mu(n_d) \end{bmatrix}, \begin{bmatrix} k(n_1, n_1) & \cdots & k(n_1, n_d) \\ \vdots & \ddots & \vdots \\ k(n_d, n_1) & \cdots & k(n_d, n_d) \end{bmatrix} \right).$$

The Gaussian process is defined by its mean function $\mu(n)$ and covariance function $k(n, n')$. We represent the GP in the following manner:

$$f(n) \sim GP(\mu(n), K(n, n')),$$

where n and n' represent any two elements within the input set \mathbf{n} . Conventionally, for the sake of simplicity, we set the mean function to zero.

The goal of Gaussian process regression is to establish a mapping between the input set \mathbf{n} and the output set θ , represented as $f(n): \mathbb{R} \rightarrow \mathbb{R}$, and to forecast the potential output value $\theta_* = f(n_*)$ at a new test point n_* . In practical linear regression scenarios, our model is given by:

$$\theta = f(n) + \eta,$$

where θ is the observed value that incorporates noise η . We presume that η adheres to a d -dimensional joint Gaussian distribution with a zero mean and variance σ^2 , that is, $\eta \sim N(0, \sigma^2)$. The common range for σ is $[10^{-6}, 10^{-2}]$. For this investigation, we have set $\sigma = 10^{-4}$.

Then, we can express the prior distribution of the observed values θ as

$$\theta \sim N(\mu_\theta(\mathbf{n}), K(\mathbf{n}, \mathbf{n}) + \sigma^2 I_d).$$

The joint prior distribution of the observed value θ and the predicted value θ_* is given by

$$\begin{bmatrix} \theta \\ \theta_* \end{bmatrix} \sim N \left(\begin{bmatrix} \mu_\theta \\ \mu_{\theta_*} \end{bmatrix}, \begin{bmatrix} K(\mathbf{n}, \mathbf{n}) + \sigma^2 I_d & K(\mathbf{n}, \mathbf{n}_*) \\ K(\mathbf{n}_*, \mathbf{n}) & K(\mathbf{n}_*, \mathbf{n}_*) \end{bmatrix} \right),$$

where I_d is the d -dimensional identity matrix, $K(\mathbf{n}, \mathbf{n}) = (k_{ij})$ is the symmetric positive definite covariance matrix, and $k_{ij} = k(n_i, n_j)$. $K(\mathbf{n}, \mathbf{n}_*)$ is the symmetric covariance matrix between the training set N and the test set \mathbf{n}_* .

According to Bayes formula, the posterior distribution of the predicted value θ_* given the observed values θ is:

$$p(\theta_* | \theta) = \frac{p(\theta | \theta_*) p(\theta_*)}{p(\theta)}, \quad (2.1)$$

where $p(\theta_*)$ is the prior distribution of the predicted value and $p(\theta)$ is the marginal likelihood of the observed values.

The joint posterior distribution of the prediction is given by:

$$\theta_* | \mathbf{n}, \theta, \mathbf{n}_* \sim N(\mu_*, \sigma_*^2), \quad (2.2)$$

where the mean μ_* and variance σ_*^2 are:

$$\begin{aligned} \mu_* &= K(\mathbf{n}_*, \mathbf{n}) [K(\mathbf{n}, \mathbf{n}) + \sigma^2 I_d]^{-1} (\theta - \mu_\theta) + \mu_{\theta_*}, \\ \sigma_*^2 &= K(\mathbf{n}_*, \mathbf{n}_*) - K(\mathbf{n}_*, \mathbf{n}) [K(\mathbf{n}, \mathbf{n}) + \sigma^2 I_d]^{-1} K(\mathbf{n}, \mathbf{n}_*). \end{aligned}$$

For the output θ_* in the test set, we use the mean of the Gaussian regression as its estimate, i.e., $\hat{\theta}_* = \mu_*$.

The kernel function plays a pivotal role in Gaussian process regression, as it is responsible for generating the covariance matrix that quantifies the similarity between any two input variables. The closer the distance between inputs, the higher the correlation between their corresponding output variables. Hence, it is essential to select or construct kernel functions that meet the specific demands of the problem at hand. Commonly utilized kernel functions include radial basis functions, rational quadratic kernel functions, exponential kernel functions, and periodic kernel functions.

In this article, we have employed a kernel learning approach. We have established a kernel function library $\mathcal{K} = \{k_\xi(x, x') | \xi = 1, \dots, N\}$, which encompasses a variety of fundamental kernel functions and their multiplicative combinations. Subsequently, we derive the kernel function by linearly combining elements from this library:

$$k(x, x') = \sum_{\xi=1}^N c_\xi k_\xi(x, x').$$

For the selection of the hyperparameter α in the kernel function, we obtain it by maximizing the log-likelihood function:

$$L = \log p(y|x, \alpha) = -\frac{1}{2} y^T [K + \sigma^2 I_d]^{-1} y - \frac{1}{2} \log [K + \sigma^2 I_d] - \frac{n}{2} \log 2\pi.$$

2.3 Multi-Indicator Driven Evaluation

In this section, we will present a comprehensive set of evaluation metrics crafted to assess the performance of Gaussian process regression, specifically in the domain of parameter prediction. These metrics offer diverse insights into the quality of the predictions, with each one reflecting different aspects of predictive performance based on their values. We will explore the details of each metric and explain how their values are indicative of the prediction model's effectiveness.

2.3.1 Positive Indicators: Value Enhancement and Prediction Optimization

In evaluating the performance of parameter predictions in Gaussian process regression, we employ a variety of metrics to thoroughly assess the model's effectiveness. This set of metrics includes the coefficient of determination R^2 , the correlation coefficient (Corr), and the Prediction Interval Coverage Probability (PICP), which together form a robust framework for measuring the model's predictive power.

The coefficient of determination, represented as R^2 , is a statistical measure that indicates the proportion of the variance in the dependent variable that can be explained by the independent variables within the regression model. It offers a measure of how well the observed outcomes are replicated by the model, relative to the total variation present in the data. The R^2 value ranges between 0 and 1, where a value of 1 indicates that the model perfectly predicts the data, and a value of 0 suggests that the model does not explain any of the variability in the response data around its mean.

The formula for calculating R^2 is as follows:

$$R^2 = 1 - \frac{\sum_{i=1}^n (y_i - \hat{y}_i)^2}{\sum_{i=1}^n (y_i - \bar{y})^2}.$$

Where y_i is the observed value of the i -th data point. \hat{y}_i is the predicted value of the i -th data point from the model. \bar{y} is the mean of the observed values. The numerator, $\sum_{i=1}^n (y_i - \hat{y}_i)^2$, corresponds to the sum of squared residuals, which measures the aggregate deviation of the data points from the model's predictions. The denominator, $\sum_{i=1}^n (y_i - \bar{y})^2$, is the total sum of squares, which signifies the overall deviation of the data points from their mean.

An elevated R^2 value indicates that the model explains a significant portion of the variance in the dependent variable. However, it is important to note that a high R^2 value does not necessarily signify an excellent model fit, as it can be influenced by the number of predictors in the model and does not account for the model's complexity or its ability to predict new, unseen data. Therefore, while R^2 is a useful measure, it should be used in conjunction with other diagnostic measures to fully assess the quality of a model's fit.

The correlation coefficient (Corr) is a statistical tool that measures the degree and direction of the linear relationship between a model's predicted values and the actual data points [30]. This coefficient is derived by dividing the covariance of the predicted and observed values by the product of their respective standard deviations, resulting in

a value that falls within the range of -1 to 1. Values nearing 1 or -1 denote a robust linear association. The formula for calculating the correlation coefficient is as follows:

$$Corr = \frac{\sum_{i=1}^n (x_i - \bar{x})(y_i - \bar{y})}{\sqrt{\sum_{i=1}^n (x_i - \bar{x})^2 \sum_{i=1}^n (y_i - \bar{y})^2}}.$$

Here, x_i and y_i represent the individual sample points indexed by i , \bar{x} and \bar{y} denote the means of the x and y values, respectively, and n is the total number of observations. The numerator of the formula calculates the covariance between the predicted and observed values, which quantifies the extent to which the variables change in tandem. The denominator is the product of the standard deviations of the two variables, which standardizes the covariance to a value that falls between -1 and 1.

The correlation coefficient is a valuable metric because it offers insight into the linear relationship between variables, unaffected by the variables' units of measurement or their scale. However, it's crucial to recognize that a high correlation coefficient does not imply causation; it signifies only a strong association between the variables. Moreover, the correlation coefficient is sensitive to outliers, making it essential to scrutinize the data for extreme values that could disproportionately affect the correlation.

Gaussian process regression not only predicts parameters but also furnishes a quantitative assessment of the uncertainty surrounding these predictions, encapsulated by the Prediction Interval Coverage Probability (PICP) [21, 25]. The PICP at a 0.95 confidence level reveals the model's capacity to ensure that true values fall within the predicted intervals. By determining the mean $\mu_*(x)$ and variance $\sigma_*^2(x)$ via Gaussian process regression, the 0.95 confidence interval can be computed as:

$$I_\theta^{0.95}(x) = [\mu_*(x) - 1.96\sigma_*(x), \mu_*(x) + 1.96\sigma_*(x)].$$

Given a test set:

$$\{x_i^{\text{test}}, i = 1, \dots, N\} \in \mathbb{X}^N,$$

where the values of z are known (actual values), the prediction interval coverage rate is:

$$PICP = \frac{1}{N} \sum_{i=1}^N \mathbf{1}_{z(x_i^{\text{test}}) \in I_\theta^{0.95}(x_i^{\text{test}})}.$$

Here, $\mathbf{1}_{z(x_i^{\text{test}}) \in I_\theta^{0.95}(x_i^{\text{test}})}$ is an indicator function that equals 1 if the actual value $z(x_i^{\text{test}})$ falls within the 95% confidence interval $I_\theta^{0.95}(x_i^{\text{test}})$, and 0 otherwise.

The PICP (Prediction Interval Coverage Probability) provides a measure of how frequently the model's predicted intervals contain the true values. A high PICP value indicates that the model's predicted intervals are reliable and include the true values a significant proportion of the time. This is a useful metric for evaluating the reliability of the model's predictions and for establishing appropriate confidence levels for the predictions.

The combined use of these performance metrics provides a comprehensive evaluation of the predictive prowess of the Gaussian process regression model. High R^2 and correlation coefficient (Corr) values indicate that the model effectively captures the underlying trends in the data. Simultaneously, a strong PICP underscores the reliability and consistency of the model's predictive outputs. This multifaceted analysis enables a deeper understanding of the model's competence in parameter prediction, offering a robust theoretical basis for informed model selection and optimization endeavors.

2.3.2 Negative Indicators: Value Reduction and Error Decrease

In the domain of assessing parameter predictions from Gaussian Process Regression (GPR) models, a suite of negative indicators is utilized to measure the magnitude of prediction errors. This collection includes Mean Squared Error (MSE), Root Mean Squared Error (RMSE) [22], Mean Absolute Error (MAE), Bayesian Information Criterion (BIC), Median Absolute Percentage Error (MdAPE), and Leave-One-Out Cross-Validated Score Error (LOO-SPE). Collectively, these metrics form a comprehensive framework for evaluating the model's predictive accuracy.

Mean Squared Error (MSE), Root Mean Squared Error (RMSE), and Mean Absolute Error (MAE) serve as direct measures of prediction error, reflecting the discrepancies between predicted values and actual observations from various perspectives. MSE assesses the model's precision by averaging the squared differences between predictions and actual values, providing a clear view of the average squared error. RMSE offers a scaled measure of error magnitude, expressed in the same units as the data, which is particularly useful for grasping the practical significance of errors. MAE provides a robust measure of error by averaging the absolute differences between predictions and actual values, making it less susceptible to the influence of outliers. In an ideal scenario, these metrics should yield lower values, signifying a higher level of predictive precision for the model.

The Bayesian Information Criterion (BIC) is a pivotal tool in model selection that imposes a penalty on model complexity to mitigate the risk of overfitting. The BIC is formulated to consider both the maximum likelihood estimate of the model and the number of parameters it contains; a lower BIC value indicates a more favorable balance between the model's fit to the data and its simplicity.

$$\text{BIC} = -2\ln(L) + k\ln(n).$$

The term $-2\ln(L)$ in the BIC formula incentivizes the model to achieve a high likelihood value, signifying a good fit to the data. Conversely, the term $k\ln(n)$ increases with the number of parameters k in the model, thus imposing a penalty for increased complexity. This aspect of the BIC ensures that models with an excessive number of parameters are penalized, even if they fit the data well, as their BIC values will be elevated. Consequently, when evaluating different models, the one exhibiting a smaller BIC value is often deemed more desirable, as it strikes a better trade-off between data fit and model

simplicity.

Within the scope of this paper, we utilize the Bayesian Information Criterion (BIC) value as a measure to evaluate the effectiveness of GPR parameter prediction. The underlying principle is that a lower BIC value indicates a superior GPR parameter prediction, implying that the model fits the data effectively while maintaining simplicity and guarding against overfitting. This method is in line with BIC's function in directing model selection towards a model that is not only efficient but also economical in its complexity.

The Median Absolute Percentage Error (MdAPE) is a robust metric for assessing the predictive accuracy of a forecasting model [33]. It measures the median of the absolute percentage differences between the predicted and actual values. The MdAPE is calculated as follows:

$$\text{MdAPE} = \text{median} \left(\left| \frac{x_i - \hat{x}_i}{x_i} \right| \right).$$

Here, x_i denotes the true value of the i -th sample, and \hat{x}_i denotes the predicted value of the i -th sample. The Median Absolute Percentage Error (MdAPE) utilizes the median instead of the mean, which makes it less sensitive to outliers, thereby offering a more dependable measure of the model's predictive performance in scenarios where extreme values are present.

In practical applications, a lower MdAPE value signifies a more precise predictive model. Typically, an MdAPE value below 0.1 is regarded as indicative of excellent predictive performance, whereas a value above 0.5 suggests poor predictive performance. This metric is especially valuable for assessing models in situations where the stakes of errors are high or where error distribution is skewed.

By integrating the MdAPE into our evaluation framework, we enhance our understanding of the model's predictive performance, particularly in terms of its resilience to outliers and its capacity to deliver accurate forecasts across various scenarios.

In addition to the previously discussed metrics, we introduce an evaluation method based on a scoring criterion known as LOO-SPE [19], which is used to assess the predictive performance of the GPR model. This method is characterized by its focus on minimizing the prediction error through the Leave-One-Out cross-validation approach. The lower the LOO-SPE value, the better the model's predictive performance is considered to be.

Within the framework of the Gaussian process regression model, the predictive distribution $P_{\theta,-i}$ is characterized by the following conditional Gaussian distribution:

$$P_{\theta,-i} \sim \mathcal{N}(\mu_{\theta_{where,-i}}, \sigma_{\theta,-i}^2),$$

$$\mu_{\theta,-i} = y_i - \frac{(C(X,X)^{-1}(y-m))_i}{(C(X,X)^{-1})_{i,i}} \quad \text{and} \quad \sigma_{\theta,-i}^2 = \frac{1}{(C(X,X)^{-1})_{i,i}}.$$

Here, $\mu_{\theta,-i}$ represents the predictive mean, $\sigma_{\theta,-i}^2$ denotes the predictive variance, and θ signifies the model parameters.

In the Leave-One-Out method, for each training sample y_i , a conditional model $P_{\theta,-i}(y|x)$ is constructed, trained on the dataset with the i -th sample excluded. The LOO-SPE scoring criterion is articulated as:

$$J_n^S(\theta) = \frac{1}{n} \sum_{i=1}^n S(P_{\theta,-i}, y_i),$$

where S is the scoring rule, and $P_{\theta,-i}$ denotes the distribution of $Y(x_i)$ given the condition $Y(x_j) = y_j$ for $j \neq i$.

We define the mean of the predictive distribution P as μ , and consider the deviation of y from μ . The squared prediction error (SPE) is given by:

$$S^{\text{SPE}}(P, y) = (y - \mu)^2.$$

Specifically, integrating the results from the Gaussian process regression model, the LOO-SPE can be articulated as:

$$J_n^{\text{SPE}}(\theta) = \frac{1}{n} \sum_{i=1}^n (\mu_{\theta,-i} - y_i)^2 = \frac{1}{n} \sum_{i=1}^n \left(\frac{(C(X, X)^{-1}(y - m))_i}{(C(X, X)^{-1})_{i,i}} \right)^2.$$

In practical applications, relying on a single metric often falls short of capturing the entire scope of a model's performance. Hence, this paper adopts a comprehensive evaluation strategy that utilizes multiple indicators to achieve a more holistic assessment of predictive performance. In the forthcoming section on numerical experiments, we will detail how these indicators can be synthesized and how they collectively enhance our understanding of the GPR model's performance in parameter prediction.

3 Numerical experiments

In this section, we focus on the role of GPR in parameter selection and provide various numerical examples to demonstrate its effectiveness. These examples not only cover a broad range of mathematical models but also showcase the performance and adaptability of GPR in various scenarios through experiments. We hope that readers can intuitively grasp the practical application value and potential advantages of GPR. To ensure the precision and credibility of the experimental results, all numerical experiments described in this section are performed by discretizing the equations using the finite element method in the IFEM software package [3], followed by solving them on the hypre platform [5]. Before the experiments begin, we perform a uniform triangulation of the computational domain to construct an appropriate numerical model. In these experiments, the iterative method is hybrid Gauss-Seidel / Jacobi, with and PMIS as the coarsening algorithm. In the pre-smoothing step, we choose the lower triangular part of matrix A_k as the smoother,

and in the post-smoothing step, we choose the upper triangular part of matrix A_k as the smoother.

We define the termination condition for our iterative process as follows:

$$tol^k = \frac{\|b - Ax^k\|_2}{\|b\|_2}.$$

Here, tol^k denotes the tolerance at the k -th iteration, b represents the known vector, A is the non-singular matrix, and x^k signifies the approximate solution at the k -th iteration. The initial tolerance is set to 0. The iterative process is halted when $tol^k < 1 \times 10^{-08}$ or when the iteration count reaches a pre-established maximum threshold, which is typically set to 200 unless otherwise indicated.

When choosing the best parameters, we focus on decreasing iterations to boost computational efficiency and numerical solution stability. If different sets yield the same iteration count, we opt for the one with the lowest error, ensuring a balance between efficiency and precision. This section uses a V-cycle approach to address linear systems.

Our numerical examples aim to highlight the practicality and performance of our GPR-based parameter selection method across various equations. We aim to showcase the GPR method's advantages in optimization, validate its theoretical basis, and underscore its robustness and effectiveness in facing real-world complexities.

3.1 Constant Coefficient Poisson Equation

We consider the constant coefficient Poisson equation, a fundamental partial differential equation in mathematical physics, given by:

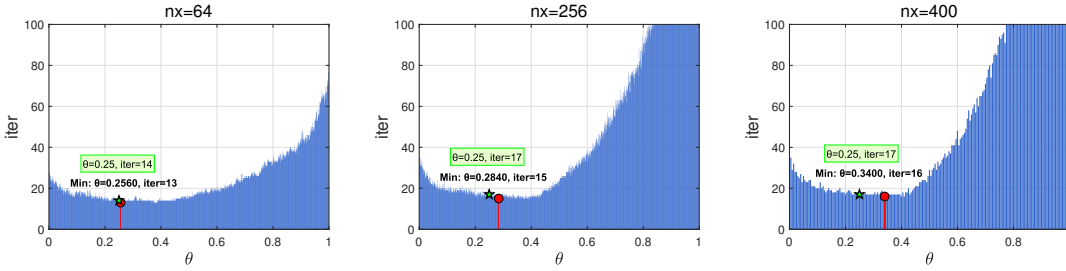
$$\begin{cases} -\nabla(a\nabla u) = f, & (x,y) \in \Omega = [0,1]^2, \\ u = 0, & (x,y) \in \partial\Omega. \end{cases}$$

Here, the coefficient $a = 1$, and the exact solution is $u = \sin(\pi x)\sin(\pi y)$. The right-hand side f is derived from the exact solution by substituting u into the Poisson equation. To find the optimal parameters for our GPR-based parameter selection method, we perform a grid search within the interval $[0,1]$ with a step size of 0.001. The number of partitions n ranges from 64 to 400 with an increment of 16. The traversal results, which identify the optimal parameters, are detailed as follows:

The subsequent figure illustrates the fluctuation in the number of iterations for the AMG method when $n = 64, 256, 400$, across various traversal parameters. The traversal for the connectivity parameter θ spans the interval $[0,1]$ with a step size of 0.001, and the iteration process is capped at a maximum of 100 iterations. The figure clearly demonstrates that the number of iterations fluctuates with changes in the connectivity parameter θ , and this fluctuation intensifies as n increases. This observation underscores the sensitivity of the AMG method's efficiency to the choice of the connectivity parameter θ .

Table 1: Traversal results of AMG solving the constant coefficient Poisson equation

n	θ	iter	n	θ	iter
64	0.256	13	240	0.268	15
80	0.269	13	256	0.284	15
96	0.387	13	272	0.267	15
112	0.324	13	288	0.287	15
128	0.222	14	304	0.311	15
144	0.246	14	320	0.275	15
160	0.293	14	336	0.285	15
176	0.352	14	352	0.319	15
192	0.351	14	368	0.314	15
208	0.334	14	384	0.349	15
224	0.232	15	400	0.34	16

Figure 1: The variation of the number of iterations for AMG solving the constant coefficient Poisson equation with different connectivity parameters θ when n is 64, 256, and 400, respectively

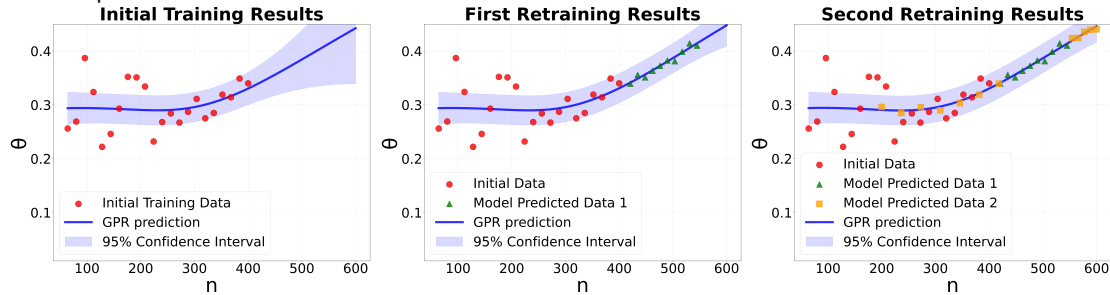
We have successfully predicted the optimal parameters for the constant coefficient Poisson equation using GPR method. The following table outlines the composition of the training set, test set, and retraining set used in our GPR model. The training set was constructed by selecting values of n from 64 to 400, with an increment of $\Delta n = 16$. For retraining we adopted targeted sampling: the first retraining phase selected 10 new points uniformly distributed in $[200,600]$, followed by a second retraining phase where 12 additional points were chosen from $[200,600]$ to refine the model further.

Table 2: Training set and retraining set for using GPR to predict the optimal parameters for AMG solving the constant coefficient Poisson equation

Training set	$n \in [64, 400], \Delta n = 16$
Retraining set 1	$n \in [200, 600]$, 10 randomly selected points
Retraining set 2	$n \in [200, 600]$, 12 randomly selected points

Table 3: Comparison of results for AMG solving the constant coefficient Poisson equation

n	predicted $\theta = 0.368$		optimal $\theta = 0.276$		$\theta = 0.25$	
	iter	time(s)	iter	time(s)	iter	time(s)
1024	17	20.4707	17	19.2373	19	21.2103

Figure 2: Regression curves for predicting θ with respect to n using GPR for AMG solving the constant coefficient Poisson equation

The following table contrasts the predicted outcomes with those acquired through the traversal method. It is clear that the difference in the number of iterations between the predicted and actual values is negligible, indicating that the predicted parameters are at least suboptimal for this specific instance. A comparison of the computational effort required to ascertain the optimal parameters via traversal versus the predictive calculations reveals that the predictive approach entails a substantially lower time cost, making it a more efficient method for parameter selection.

The subsequent tables provide a comparative analysis of predictive accuracy for various kernel function combinations in the context of parameter prediction for the constant coefficient Poisson equation. The results indicate that the combined Gaussian and Laplacian kernel function outperforms the single Gaussian kernel across multiple evaluation metrics related to parameter prediction. Remarkably, except for the combination of rational quadratic and Gaussian kernel functions, which have lower Prediction Interval Coverage Probability (PICP), the PICP values for all other combined kernel functions are at least as high as those of the single Gaussian kernel. This suggests that using multiple kernel functions can lead to a more robust predictive model.

This observation highlights the significant advantage of using combined kernel functions to enhance the predictive capabilities of the GPR model. The fact that PICP values are maintained at or above those of the single Gaussian kernel implies that the combined kernel approach does not sacrifice the reliability of predictions, while also potentially enhancing other predictive performance aspects.

The superior performance of the combined kernel function, especially in the context of parameter prediction for the constant coefficient Poisson equation, underscores its potential for providing more accurate and reliable predictions. This insight is vital for the development of GPR models that can effectively handle the complexities of real-

world applications, where the selection of the kernel function can substantially affect the model's predictive prowess.

Table 4: Evaluation of kernel function combinations for the constant coefficient Poisson equation

Kernel function	MSE	RMSE	MAE	R ²	BIC	Corr	MdAPE	LOO-SPE
Gaussian+Laplacian	4.4889×10^{-4}	0.0211	0.0193	0.3965	-250.2432	0.7294	0.0708	4.6958×10^{-4}
Gaussian+Exponential	8.0597×10^{-4}	0.0283	0.0265	0.0834	-262.6505	0.4165	0.1092	5.1552×10^{-4}
Gaussian	5.4078×10^{-4}	0.0232	0.0179	0.2730	-344.3922	0.6799	0.0421	4.7050×10^{-5}
Rational Quadratic+Laplacian	1.8333×10^{-3}	0.0428	0.0334	0.0464	-550.7246	0.7820	0.0976	1.6778×10^{-4}
Matérn+Laplacian	4.6227×10^{-4}	0.0215	0.0198	0.3785	-245.4437	0.7207	0.0743	4.8102×10^{-4}
Rational Quadratic+Gaussian	7.7147×10^{-4}	0.0277	0.0261	0.0370	-259.8924	0.6199	0.1024	6.3889×10^{-4}
Matérn+Gaussian+Laplacian	4.6351×10^{-4}	0.0215	0.0198	0.3769	-232.9368	0.7208	0.0743	4.8336×10^{-4}

Table 5: PICP evaluation for the constant coefficient Poisson equation

Kernel function	PICP
Gaussian+Laplacian	100.0 %
Gaussian+Exponential	100.0 %
Gaussian	57.1 %
Rational Quadratic+Laplacian	42.9 %
Matérn+Laplacian	100.0 %
Rational Quadratic+Gaussian	57.1 %
Matérn+Gaussian+Laplacian	100.0 %

3.2 2D Diffusion Equation

We consider the following two-dimensional diffusion equation, derived from [34]:

$$\begin{aligned} -\nabla \cdot (\kappa \nabla u) &= f_1, & x \in \Omega, \\ u &= f_2, & x \in \partial\Omega \end{aligned} \quad (3.1)$$

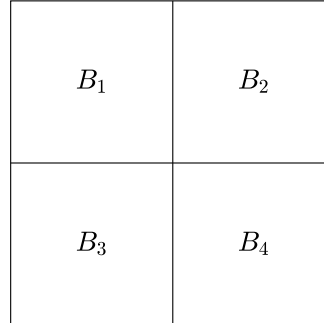
The domain is $[0,1]^2$, and the diffusion coefficients are

$$\kappa = \begin{bmatrix} 10^{Mr_0} & 0 \\ 0 & 10^{Mr_1} \end{bmatrix}.$$

where r_0, r_1 are random numbers in the interval $(0,1)$. The positive number M will influence the multiscale properties of the matrix.

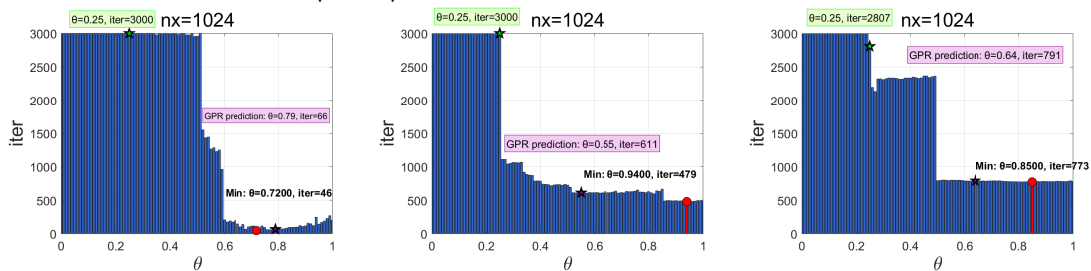
During the discretization process, the computational domain is uniformly divided into T^2 blocks based on the partition number T , as illustrated in Figure 2. The diffusion coefficient κ remains constant within each block but varies across different blocks. Consequently, even with fixed discretization parameter n and partition number T , different random seeds will yield different matrices.

Figure 3: When $T=2$, the computational domain is uniformly partitioned into four blocks ($B_i, i=1,2,3,4$). Diffusion coefficient κ is the same in each block, when $B_i \neq B_j, k_i \neq k_j$.



Specifically, we generate the training set starting from $n = 64$ with a step size of 16 until $n = 400$. For each matrix generation, T randomly varies within the interval $(10,20)$, and the random seed is equal to the index of the matrix. We will now conduct three sets of experiments. For each set, the training set consists of 23 matrices, and we will test them using matrices of size $n_x = 1024$. The three sets of experimental traversal graphs below compare iteration steps under three configurations: optimal parameters, default parameters, and GPR-predicted parameters. To further validate the precision of GPR predictions, Table reft2dks summarizes the average iteration steps and CPU time across these parameters. Results show that the GPR-predicted parameters reduce computational costs compared to default values while closely approximating the optimal parameters' efficiency.

Figure 4: Traversal plots for three sets of test matrices, along with iteration steps corresponding to GPR prediction, default values, and optimal parameters



3.3 Helmholtz Equation

We have delved into the two-dimensional Helmholtz equation, a milestone partial differential equation in physics and engineering. The Helmholtz equation is widely recog-

Table 6: Test results of 2D diffusion equations

n	optimal θ		$\theta = 0.25$		GPR prediction	
	iter	time(s)	iter	time(s)	iter	time(s)
1024	432.67	51.1676	935.67	178.8975	489.34	78.8897

nized for its significant role in modeling wave propagation phenomena, as it can describe the propagation characteristics of waves in various media, including sound waves, light waves, and other types of waves. This equation is not only central to theoretical research but also extremely important in practical applications, such as in acoustics, optics, electromagnetism, and quantum mechanics. The mathematical expression of this equation is as follows:

$$\begin{cases} \Delta u + k^2 u = f, & (x, y) \in \Omega = (-1, 1)^2, \\ u(-1, y) = u(1, y) = 0, & y \in (-1, 1), \\ u(x, -1) = u(x, 1) = -\sin(\pi x), & x \in (-1, 1). \end{cases}$$

The exact solution to this equation is $u = \sin(\pi x) \cos(\pi y)$, and the corresponding right-hand side term is $f = (k^2 - \pi^2) \sin(\pi x) \cos(\pi y)$.

In this particular scenario, we assign the wave number k a value of 2π . The connectivity parameter is systematically traversed with an increment of 0.001 across the interval $[0, 1]$, while the number of partitions n spans from 64 to 400, incrementing by 16 for each step. The detailed traversal outcomes are presented in Table 7.

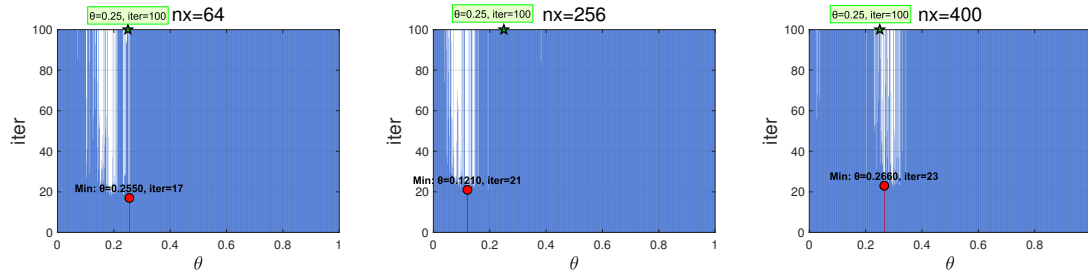
Table 7: Traversal results of AMG solving the Helmholtz equation with coefficient 2π

n	θ	iter	n	θ	iter
64	0.255	17	240	0.139	20
80	0.414	19	256	0.121	21
96	0.108	20	272	0.142	21
112	0.083	22	288	0.094	23
128	0.032	31	304	0.096	23
144	0.260	21	320	0.066	24
160	0.239	20	336	0.068	23
176	0.204	20	352	0.275	22
192	0.250	20	368	0.328	22
208	0.155	20	384	0.344	22
224	0.160	20	400	0.266	23

Proceeding further, we present the variation in the number of iterations for the AMG method as the traversal parameters are altered, with the number of subdivisions n specified as 64, 256, 400. The connectivity parameter is traversed over the interval $(0, 1]$ with a step size of 0.001, and the iteration process is limited to a maximum of 100 iterations.

These findings offer valuable insights into the impact of the connectivity parameter selection on the performance of the AMG method across various spatial discretization levels.

Figure 5: Variation of the number of iterations for AMG solving the Helmholtz equation with coefficient 2π and different connectivity parameters θ when n is 64,256,400, respectively



Below, we forecast the optimal parameters for the AMG method when solving the Helmholtz equation using GPR method. Table 3.3 presented details of the training set, and retraining set for GPR. The training set is derived by selecting n values from 64 to 400, incrementing by $\Delta n = 16$. For retraining we adopted targeted sampling: the first retraining phase selected 10 new points uniformly distributed in $[200,600]$, followed by a second retraining phase where 12 additional points were chosen from $[200,600]$ to refine the model further.

Table 8: Training set, test set, and retraining set for using GPR to predict the optimal parameters for AMG solving the Helmholtz equation with coefficient 2π

Training set	$n \in [64,400], \Delta n = 16$
Test set	$n \in [200,600], 10$ randomly selected points
Retraining set	$n \in [200,600], 12$ randomly selected points

Continuing, we depict the regression curve that illustrates the relationship between the connectivity parameter θ and the number of partitions n in the AMG method as predicted by GPR. The green regions within the figure denote the confidence intervals, signifying that the predicted results have a significant degree of reliability.

Figure 6: Regression curves of θ with respect to n predicted by GPR for AMG solving the Helmholtz equation with coefficient 2π

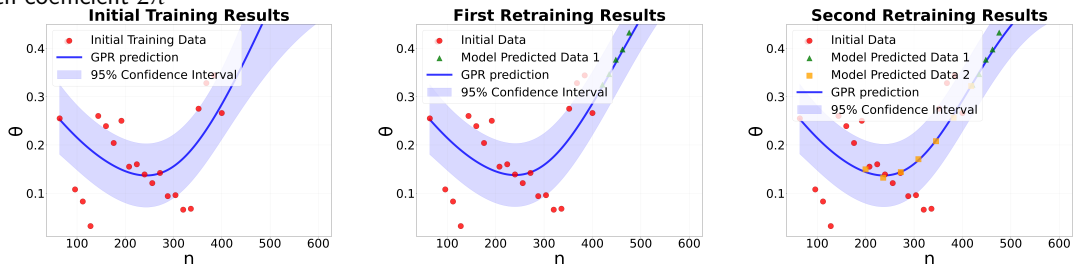


Table 9: Comparison of results for AMG solving the Helmholtz equation with coefficient 2π

n	predicted $\theta = 0.344$		optimal $\theta = 0.323$		$\theta = 0.25$	
	iter	time(s)	iter	time(s)	iter	time(s)
1024	27	55.5796	25	51.0620	non-convergence	non-convergence

Table 3.3 list the result of the iteration counts and CPU time under three parameter selection schemes for the case of $n=1024$, where optimal θ is the traversal-derived parameter. The parameters predicted by the Gaussian Process Regression (GPR) model not only closely match those obtained from the exhaustive search method, but also demonstrate high accuracy. This consistency validates the reliability of the GPR prediction approach, which can approximate the computational results of exhaustive search with remarkable precision.

The Table 3.3 and 3.3 provide a comparative analysis of the predictive accuracy achieved by various combinations of kernel functions when applied to the Helmholtz equation with the coefficient $k = 2\pi$. The results indicate that the combination of the Rational Quadratic kernel function and the Laplacian kernel function stands out, exhibiting the lowest Median Absolute Percentage Error (MdAPE) and the lowest Mean Squared Error (MSE). Additionally, with the exception of the final set of combined kernel function parameters, which shows a slightly lower Prediction Interval Coverage Probability (PICP), all other combinations achieve a perfect interval coverage rate of 100%. This underscores the effectiveness and superiority of the Rational Quadratic-Laplacian kernel combination in this context.

Table 10: Evaluation of kernel function combinations for Helmholtz equation with coefficient 2π

Kernel function	MSE	RMSE	MAE	R ²	BIC	Corr	MdAPE	LOO-SPE
Gaussian+Laplacian	5.9361×10^{-3}	0.0770	0.0652	0.0461	-150.6211	0.9271	0.3080	2.3634×10^{-3}
Gaussian+Exponential	9.1618×10^{-3}	0.0957	0.0802	0.0255	-153.9052	0.7689	0.3347	2.8059×10^{-3}
Gaussian	3.9714×10^{-3}	0.0630	0.0526	0.0224	-251.7541	0.6933	0.2432	2.3984×10^{-4}
Rational Quadratic+Laplacian	3.6738×10^{-3}	0.0606	0.0442	0.0957	-377.5221	0.7645	0.1425	2.2405×10^{-2}
Matérn+Laplacian	6.4141×10^{-3}	0.0801	0.0673	0.5787	-145.9441	0.9307	0.3139	2.4222×10^{-3}
Rational Quadratic+Gaussian	4.6182×10^{-3}	0.0679	0.0612	0.0136	-155.5238	0.9437	0.2517	2.2826×10^{-3}
Matérn+Gaussian+Laplacian	6.5222×10^{-3}	0.0807	0.0679	0.0605	-137.4683	0.9326	0.3152	2.4398×10^{-3}

Table 11: PICP evaluation for the Helmholtz equation with coefficient 2π

Kernel function	PICP
Gaussian+Laplacian	85.7 %
Gaussian+Exponential	85.7 %
Gaussian	42.9 %
Rational Quadratic+Laplacian	28.6%
Matérn+Laplacian	71.4 %
Rational Quadratic+Gaussian	85.7 %
Matérn+Gaussian+Laplacian	85.7 %

4 Summary

In this paper, we have highlighted the effectiveness of kernel learning methods, particularly GPR, in optimizing parameters for AMG when solving various PDEs. The results demonstrated significant time savings and high reliability in parameter prediction, especially when using combined kernel functions. These findings provided valuable theoretical support for AMG optimization and practical applications.

In future, there are three promising directions worth exploring. First, mixed precision computing can be integrated with GPR-based AMG optimization. By leveraging low-precision computations for initial parameter exploration and high-precision adjustments for accuracy, computational efficiency can be further enhanced. Second, extending this approach to more complex PDEs, such as nonlinear equations and multiphysics problems, will require developing advanced kernel functions and multitask learning frameworks to handle their nonlinearity and multiscale nature. This extension could significantly improve the efficiency and accuracy of solving these challenging problems. Third, we will consider to employ Online Gaussian Process Regression (Online GPR) to address the challenges of few-shot learning and dynamic adaptation in large-scale matrix parameter prediction. This method utilizes an incremental learning mechanism to achieve dynamic optimization and real-time updating of model parameters, effectively overcoming the parameter adjustment latency inherent in traditional batch processing methods when handling streaming data.

In conclusion, the integration of kernel learning with AMG parameter optimization offers a promising path forward. Future work on mixed precision techniques and complex PDEs will likely yield more efficient and reliable numerical methods for solving real-world scientific and engineering problems.

Acknowledgments

The author would like to thank The National Key R&D Program of China (2023YFB3001604) and expresses sincere gratitude for its support and assistance to our work.

References

- [1] Antonietti P F, Caldana M, Dede' L. Accelerating algebraic multigrid methods via artificial neural networks. *Vietnam Journal of Mathematics*, 51 (2023), pp. 1-36.
- [2] Antonietti P F, Melas L. Algebraic multigrid schemes for high-order nodal discontinuous Galerkin methods. *SIAM Journal on Scientific Computing*, 42 (2020), pp. A1147-A1173.
- [3] Chen L. iFEM: an innovative finite element methods package in MATLAB. Preprint, University of Maryland, 20, (2008).
- [4] C K I Williams, C E Rasmussen. *Gaussian processes for machine learning*. Cambridge, MA: MIT press, (2006)

- [5] Falgout R D, Yang U M. hypre: A library of high performance preconditioners. International Conference on computational science. Berlin, Heidelberg: Springer Berlin Heidelberg, (2002),pp. 632-641.
- [6] Gronau Q F, Wagenmakers E J. Limitations of Bayesian leave-one-out cross-validation for model selection. *Computational Brain & Behavior*, 2 (2019), pp. 1-11.
- [7] Gottschalk H, Kahl K. Coarsening in algebraic multigrid using Gaussian processes. *Electronic Transactions on Numerical Analysis*, 54 (2021), pp. 514-533.
- [8] Haghi P, Geng T, Guo A, Wang T, Herbordt M. FP-AMG: FPGA-based acceleration framework for algebraic multigrid solvers. In: 2020 IEEE 28th Annual International Symposium on Field-Programmable Custom Computing Machines (FCCM), 2020, pp. 148-156.
- [9] Hodson T O. Root mean square error (RMSE) or mean absolute error (MAE): When to use them or not. *Geoscientific Model Development Discussions*, 2022, pp. 1-10.
- [10] Jiang K, Su X, Zhang J. A general alternating-direction implicit framework with Gaussian process regression parameter prediction for large sparse linear systems. *SIAM Journal on Scientific Computing*, 44 (2022), pp. A1960-A1988.
- [11] Jiang K, Zhang J, Zhou Q. Multitask kernel-learning parameter prediction method for solving time-dependent linear systems. *CSIAM Transactions on Applied Mathematics*, 4 (2023), pp. 672-695.
- [12] Kickinger F. Algebraic multi-grid for discrete elliptic second-order problems. In: *Multigrid Methods V: Proceedings of the Fifth European Multigrid Conference held in Stuttgart, 1998*, pp. 157-172.
- [13] Ruge J W, Stüben K. Algebraic multigrid. In: *Multigrid Methods*, 1987, pp. 73-130.
- [14] Richter C, Schöps S, Clemens M. GPU acceleration of algebraic multigrid preconditioners for discrete elliptic field problems. *IEEE Transactions on Magnetics*, 50 (2014), pp. 461-464.
- [15] Luz I, Galun M, Maron H, Basri R, Yavneh I. Learning algebraic multigrid using graph neural networks. In: *International Conference on Machine Learning*, 2020, pp. 6489-6499.
- [16] Brezina M, Falgout R, MacLachlan S, McCormick T, McCormick S, Ruge J. Adaptive algebraic multigrid. *SIAM Journal on Scientific Computing*, 27 (2006), pp. 1261-1286.
- [17] Neath A A, Cavanaugh J E. The Bayesian information criterion: background, derivation, and applications. *Wiley Interdisciplinary Reviews: Computational Statistics*, 4 (2012), pp. 199-203.
- [18] Bastian P, Blatt M, Scheichl R. Algebraic multigrid for discontinuous Galerkin discretizations of heterogeneous elliptic problems. *Numerical Linear Algebra with Applications*, 19 (2012), pp. 367-388.
- [19] Petit S J, Bect J, Feliot P, Vazquez E. Parameter selection in Gaussian process interpolation: an empirical study of selection criteria. *SIAM/ASA Journal on Uncertainty Quantification*, 11 (2023), pp. 1308-1328.
- [20] Rad K R, Maleki A. A scalable estimate of the out-of-sample prediction error via approximate leave-one-out cross-validation. *Journal of the Royal Statistical Society Series B: Statistical Methodology*, 82 (2020), pp. 965-996.
- [21] Rahmati O, Choubin B, Fathabadi A, Coulon F, Soltani E, Shahabi H, ... & Bui D T. Predicting uncertainty of machine learning models for modelling nitrate pollution of groundwater using quantile regression and UNEEC methods. *Science of the Total Environment*, 688 (2019), pp. 855-866.
- [22] Ranjan R, Huang B, Fatehi A. Robust Gaussian process modeling using EM algorithm. *Journal of Process Control*, 42 (2016), pp. 125-136.
- [23] Sbai M A, Larabi A. On solving groundwater flow and transport models with algebraic

- multigrid preconditioning. *Groundwater*, 59 (2021), pp. 100-108.
- [24] Schulz E, Speekenbrink M, Krause A. A tutorial on Gaussian process regression: Modelling, exploring, and exploiting functions. *Journal of Mathematical Psychology*, 85 (2018), pp. 1-16.
 - [25] Shrestha D L, Solomatine D P. Machine learning approaches for estimation of prediction interval for the model output. *Neural Networks*, 19 (2006), pp. 225-235.
 - [26] Taghibakhshi A, MacLachlan S, Olson L, West M. Optimization-based algebraic multigrid coarsening using reinforcement learning. *Advances in Neural Information Processing Systems*, 34 (2021), pp. 12129-12140.
 - [27] Vehtari A, Gelman A, Gabry J. Practical Bayesian model evaluation using leave-one-out cross-validation and WAIC. *Statistics and Computing*, 27 (2017), pp. 1413-1432.
 - [28] Watanabe S. A widely applicable Bayesian information criterion. *The Journal of Machine Learning Research*, 14 (2013), pp. 867-897.
 - [29] Wiesner T A, Mayr M, Popp A, Gee M W, Wall W A. Algebraic multigrid methods for saddle point systems arising from mortar contact formulations. *International Journal for Numerical Methods in Engineering*, 122 (2021), pp. 3749-3779.
 - [30] Wan X, Li X, Wang X, Yi X, Zhao Y, He X, ... & Huang M. Water quality prediction model using Gaussian process regression based on deep learning for carbon neutrality in paper-making wastewater treatment system. *Environmental Research*, 211 (2022), pp. 112942.
 - [31] Notay Y. An aggregation-based algebraic multigrid method. *Electronic Transactions on Numerical Analysis*, 37 (2010), pp. 123-146.
 - [32] Ye S, Xu X, An H, Yang X. A supplementary strategy for coarsening in algebraic multigrid. *Applied Mathematics and Computation*, 394 (2021), pp. 125795.
 - [33] Yadav A, Bareth R, Kochar M, Pazoki M, Sehiemy R A E. Gaussian process regression-based load forecasting model. *IET Generation, Transmission & Distribution*, 18 (2024), pp. 899-910.
 - [34] Zou H, Xu X, Zhang C S, Mo Z Y. AutoAMG (θ): An Auto-tuned AMG Method Based on Deep Learning for Strong Threshold. *Communications in Computational Physics*, 36 (2024), pp. 200-220.